
A NEW PERSPECTIVE TO FISH TRAJECTORY IMPUTATION: A METHODOLOGY FOR SPATIOTEMPORAL MODELING OF ACOUSTICALLY TAGGED FISH DATA

A PREPRINT

✉ **Mahshid Ahmadian***

Department of Statistical Sciences and Operations Research
Virginia Commonwealth University
Richmond, VA 23220

Edward L. Boone

Department of Statistical Sciences and Operations Research
Virginia Commonwealth University
Richmond, VA 23220

Grace S. Chiu

William & Mary's Virginia Institute of Marine Science
Gloucester Point, VA 23062
and
Department of Statistical Sciences and Operations Research
Virginia Commonwealth University
Richmond, VA 23220

ABSTRACT

The focus of this paper is a key component of a methodology for understanding, interpolating, and predicting fish movement patterns based on spatiotemporal data recorded by spatially static acoustic receivers. For periods of time, fish may be far from the receivers, resulting in the absence of observations. The lack of information on the fish's location for extended time periods poses challenges to the understanding of fish movement patterns, and hence, the identification of proper statistical inference frameworks for modeling the trajectories. As the initial step in our methodology, in this paper, we implement an imputation strategy that relies on both Markov chain and Brownian motion principles to enhance our dataset over time. This methodology will be generalizable and applicable to all fish species with similar migration patterns or data with similar structures due to the use of static acoustic receivers.

Keywords Animal movement, Spatiotemporal data, Missing not at random

1 Introduction

Significant emphasis has been put on the study and modeling of spatiotemporal data over the years. In particular, modeling animal movement over time across a spatial landscape has gained considerable attention. For example, investigating the displacements of marine animals in water is crucial for advancing marine science, particularly understanding the population dynamics of various fish species and the effects on environmental and ecosystem conditions due to fishing practices. The structure of datasets in this type of research highly depends on the data collection method. Indeed, statistical methodology that can generate useful predictions has been lacking for complex

*Corresponding author. ahmadianm@vcu.edu

data structures like ours. This poses challenges that are not readily addressed by common methods, as we explain in section 2.

Previous research has employed diverse approaches for modeling animal movement data, such as agent-based models [10, 19, 4], Lévy flight models [21, 9], state-space models [5, 13, 14, 18], Markov models [16, 20], hidden Markov models [15, 17], functional data models [6, 7], and generalized additive models [2]. Each approach has its own benefits and limitations. For example, agent-based models (ABMs) have been widely used, especially by ecologists and environmental scientists, to simulate the actions and interactions of individual agents (fish, in our case), and assess their effects on the population. Lévy flight models involve random walks that incorporate a heavy-tailed distribution for each defined step. State-space models use latent and observed states probabilistically. They are often used in time series forecasting, economic indicators, and tracking and navigation. These models have been used in the study of animal movement because they are very effective in handling incomplete data, where animals are partially observed through receivers or satellites. Moreover, hidden Markov models extend the Markov model by incorporating hidden states that represent unobserved steps in an animal movement process. Functional data models are valuable in capturing the dynamics of animal movements by considering the movement data as realizations of continuous functions; this helps to reveal patterns that traditional approaches may miss. Generalized additive models (sometimes expressed as functional data models) are used to investigate complex animal behaviors and movement patterns by offering a flexible approach to modeling non-linear relationships between animal movement and environmental factors.

The purpose of this paper is to propose a new method for imputing animal trajectories, particularly when the data are collected using acoustic receivers. Many existing methods for imputing unobserved locations in a trajectory rely on observed locations. However, in our case where data are collected using sparsely located, spatially static acoustic receivers so that the exact location of the animal is unavailable much more often than not, a new methodology is needed. For our proposed approach, the updated direction of fish movement at each step and the remaining distance until the next observed location are two key components in the movement model.

The organization of this paper is as follows: Section 2 introduces the dataset that we used for this study and it highlights the challenges posed by the dataset structure. Section 3 delves into the algorithm followed by section 4 that discusses the likelihood associated with our method. In section 5, we present a simulation study and the visual results of the proposed algorithm. Finally, section 6 outlines the next steps and potential directions for future research.

2 Data

Methods for analyzing environmental data may vary across datasets, influenced not only by the nature of the scientific problem but also by the methods of data collection. Our research is tailored to a specific dataset by [2] that provides information on fish movement along the US East Coast. The data, collected from 2014 to 2020, utilize acoustic tagging of a species known as cobia (*Rachycentron canadum*) in the Atlantic waters and include details such as the GPS coordinates of the spatially static acoustic receivers and the corresponding time stamp of the detection of a tagged fish. It is important to emphasize that the only spatial information available on each fish is whether or not it was in a receiver’s detection range ($\sim 500m$), and hence, the precise location of the individual fish is not available. Instead, the GPS coordinates of the receivers around which the fish was swimming and was detected is the only spatial information available. Furthermore, this sensing regime implies that no information is available when the fish is swimming outside the detection area of the network of embedded receivers.

Other studies on cobia have employed various techniques to understand their movement patterns and habitat utilization. Pop-up satellite archival tags (PSATs) have been used to assess the post-release survival, net travel distance, and habitat utilization of cobia in Virginia waters, providing valuable data on their movements and behavior [12]. But the study of fish movement has been completely transformed by acoustic tagging technology. These tags emit a sound signal that is recognizable by the underwater receivers, helping ecologists track tagged marine animals. In many scenarios where the traditional tracking methods, such as satellites, are not effective, the use of acoustic receivers is valuable [11]. However, this technology has its own challenges, which include high costs, behavioral impacts on animals, and data gaps and missingness caused by reasons such as environmental noise or tag failure [22, 1, 8], in addition to the sparsity (due to high costs) and static nature of receivers being used to monitor highly mobile animals.

3 Method

This section describes our probability model. The complexity of the data, as discussed above, creates a two-fold problem due to acoustic tagging: the imprecise location of any detected fish and a high abundance of gaps in the location of the fish. We implement an imputation strategy that relies on both Markov chain and Brownian motion principles to enhance the comprehensiveness of our dataset over time.

Consider the movement trajectory of one fish, and let X_{jt} be the bivariate vector of longitude and latitude of the location of fish j at time step t , where $j = 1, \dots, J$, and $t = 1, 2, 3, \dots$. Further, let

$$X_{jt} = \begin{cases} M_{jt} & \text{fish } j \text{ location at } t \in \tau_{M_j} \\ N_{jt} & \text{fish } j \text{ location at } t \in \tau_{N_j} \end{cases} \quad (1)$$

where τ_{N_j} is the set of time steps in which fish j is observed by a receiver, and τ_{M_j} is the set of time points when the fish is out of detection range ($\tau_{N_j} \cup \tau_{M_j}$ covers all time points). Thus, M_{jt} is the coordinates of fish j beyond the detection radius r (taken to be 500m) of any receiver, and N_{jt} is the coordinates of fish j within the detection radius r of some receiver. Thus, letting R_i denote the coordinates of receiver i , we have the constraints

$$\|N_{jt} - R_i\| \leq r \quad \text{for some } i \quad \text{and} \quad \|M_{jt} - R_i\| > r \quad \text{for all } i = 1, \dots, I$$

Imputing the location of the fish for times $t \in \tau_{N_j}$ is to pick a random point from a circular cloud of points centered at the receiver's coordinates, where the density of points decreases as the fish moves away from the center. Hence, we assume the bivariate normal distribution

$$N_{jt} \sim \mathbf{N}_2(R_i, \Sigma_R), \quad \text{for some } i \quad (2)$$

in which the covariance matrix is defined as:

$$\Sigma_R = \begin{bmatrix} \sigma_R^2 & 0 \\ 0 & \sigma_R^2 \end{bmatrix}. \quad (3)$$

This means that the imputed coordinates of the fish within the detection radius of a receiver are normally distributed with an equal variance of σ_R^2 in any direction around the receiver.

However, for the time steps of $t \in \tau_{M_j}$, we use a more complex model that incorporates direction and distance. This approach is tailored to the movement characteristics of each fish and ensures that the fish moves toward the final location in a logical time frame, as follows.

Consider fish j during an unobserved period of time between observations at $t = 1$ and $t = T_j$. That is, receivers detected fish j at times 1 and T_j , but not at $t = 2, 3, \dots, T_j - 1$. By letting θ_{jt} be the angle between the fish's imputed location at time $t - 1$ and its final location, say $X_{jT_j} = X_j^*$ imputed by equations 2 - 3, the location at each step t for $t = 2, 3, \dots, T_j - 1$ is modeled as

$$M_{jt} = X_{j(t-1)} + \begin{bmatrix} |D_{jt}| \cos(\theta_{jt} + \psi_{jt}) \\ |D_{jt}| \sin(\theta_{jt} + \psi_{jt}) \end{bmatrix}, \quad (4)$$

where

$$\begin{aligned} D_{jt} &\sim \mathcal{N}\left(\frac{d_{jt}}{T_j - (t - 1)}, d_{jt}^\phi\right), \quad \psi_{jt} \sim \mathcal{N}(0, \sigma_{\psi_{jt}}^2), \\ d_{jt} &= \|X_j^* - X_{j(t-1)}\| - 2r, \\ \sigma_{\psi_{jt}}^2 &= \begin{cases} \gamma \cdot \exp(\alpha(n_j - (t - 1))) & n_j \leq \beta \\ \gamma \cdot U & n_j > \beta, \end{cases} \end{aligned} \quad (5)$$

and $n_j = T_j - 2$ is the total number of unobserved time steps. Below is the rationale for these assumptions.

To accurately account for the distance traveled at each time step, we model D_{jt} as normally distributed where the mean is defined to ensure the imputation process considers the remaining distance. Here, d_{jt} represents the total distance that remains to be traveled from time t minus the two receivers' radii. Additionally, the variance is modeled using a power decay function to capture variability in the remaining distance traveled where ϕ is a parameter that controls the decay rate of variance with respect to the remaining distance. (This is a decay function because d_{jt} decreases as t increases.) This formulation ensures that both the mean and the variance dynamically adjust based on the remaining distance, providing a robust framework for imputing missing location in a spatiotemporal context.

Moreover, to incorporate a direction of movement, the γ in equation 5 represents the initial value of the variance of the noise term ψ_{jt} , and α is a parameter that controls the exponential decay of the variance. The threshold β determines the point at which the variance model switches from exponential to a uniform distribution, where $U \sim \text{Uniform}(0, 1)$. This assumption implies that for smaller gaps ($n_j \leq \beta$) the variance decreases exponentially as the fish moves toward the end point of its trajectory. However for larger time gaps ($n_j > \beta$) we give extra freedom to ψ_{jt} by considering a variance value derived from the uniform distribution.

4 Likelihood

In this section, we derive the likelihood by breaking it down into small steps. Let's consider fish j and one segment of this fish trajectory which started at $t = 1$ and ended at $t = T_j$. Thus, we drop the subscript j from the following equations.

According to equation 1, $\forall t \in \tau_N = \{1, T\}$,

$$X_t = \begin{bmatrix} X_t^{(1)} \\ X_t^{(2)} \end{bmatrix} \sim \mathbf{N}_2(R_t, \Sigma_R)$$

where

$$R_t = \begin{cases} R_i & \text{if receiver } i \text{ detected the fish at time } t \\ \text{NA} & \text{otherwise.} \end{cases}$$

Therefore, the joint density of X_1 and X_T is defined as

$$\mathcal{P}_0(X_1, X_T | R_1, R_T, \sigma_R^2) = \left(\frac{1}{2\pi\sigma_R^2} \right)^2 \exp \left(-\frac{1}{2\sigma_R^2} \sum_{t=1, T} [(X_t^{(1)} - R_t^{(1)})^2 + (X_t^{(2)} - R_t^{(2)})^2] \right).$$

Let t belong to the set $\tau_M = \{2, 3, \dots, T-1\}$, and $\mathbf{Z}_t = \begin{bmatrix} \cos(\theta_t^*) \\ \sin(\theta_t^*) \end{bmatrix}$, for $\theta_t^* = \theta_t + \psi_t$; hence,

$$\theta_t^* | \theta_t, \sigma_{\psi_t}^2 \sim \mathcal{N}(\theta_t, \sigma_{\psi_t}^2).$$

By using a two-term Taylor expansion of $\mathbf{Z}_t = \mathbf{Z}_t(\theta_t^*)$ around θ_t , we have (see Appendix A)

$$\mathbf{Z}_t | \theta_t, \sigma_{\psi_t}^2 \stackrel{approx}{\sim} \mathbf{N}_2(\boldsymbol{\mu}_z, \Sigma_z)$$

where

$$\boldsymbol{\mu}_z = \begin{bmatrix} \cos(\theta_t) - \frac{1}{2} \cos(\theta_t) \sigma_{\psi_t}^2 \\ \sin(\theta_t) - \frac{1}{2} \sin(\theta_t) \sigma_{\psi_t}^2 \end{bmatrix},$$

and letting $C_t = \cos(\theta_t)$ and $S_t = \sin(\theta_t)$, the covariance matrix is

$$\Sigma_z = \sigma_{\psi_t}^2 \begin{bmatrix} S_t^2 + \frac{1}{2} C_t^2 \sigma_{\psi_t}^2 & -S_t C_t + \frac{1}{2} S_t C_t \sigma_{\psi_t}^2 \\ -S_t C_t + \frac{1}{2} S_t C_t \sigma_{\psi_t}^2 & C_t^2 + \frac{1}{2} S_t^2 \sigma_{\psi_t}^2 \end{bmatrix}.$$

Next, let $\mathbf{W}_t = |D_t| \mathbf{Z}_t$, thus

$$\mathbf{W}_t | D_t, \theta_t, \sigma_{\psi_t}^2 \stackrel{approx}{\sim} \mathbf{N}_2(|D_t| \boldsymbol{\mu}_z, D_t^2 \Sigma_z).$$

Letting $X_t = X_{t-1} + W_t$, we have,

$$X_t | X_{t-1}, D_t, \theta_t, \sigma_{\psi_t}^2 \stackrel{approx}{\sim} \mathbf{N}_2(X_{t-1} + |D_t| \boldsymbol{\mu}_z, D_t^2 \Sigma_z)$$

with density

$$\begin{aligned} \mathcal{P}_1(X_t | X_{t-1}, D_t, \theta_t, \sigma_{\psi_t}^2) &= \\ \frac{1}{2\pi D_t^2 |\Sigma_z|^{1/2}} \exp \left(-\frac{1}{2} (X_t - X_{t-1} - |D_t| \boldsymbol{\mu}_z)^T (D_t^2 \Sigma_z)^{-1} (X_t - X_{t-1} - |D_t| \boldsymbol{\mu}_z) \right). \end{aligned}$$

Next, as ϕ is non-stochastic, we have $D_t | d_t, \phi \sim \mathcal{N}(\frac{d_t}{T - (t-1)}, d_t^\phi)$ with density

$$\mathcal{P}_2(D_t | d_t, \phi) = \frac{1}{\sqrt{2\pi d_t^\phi}} \exp \left(-\frac{1}{2 d_t^\phi} \left(D_t - \frac{d_t}{T - (t-1)} \right)^2 \right).$$

Note that conditioned on X_{t-1} and X^* , both d_t and θ_t are non-stochastic, and depending on n_j , $\sigma_{\psi_t}^2$ is either non-stochastic or has a uniform distribution. Thus, the joint distribution of stochastic terms relevant to time $t \in \tau_M$ is:

$$\begin{aligned} f(X_t, X_{t-1}, X_1, X^*, D_t, d_t, \theta_t) &= \\ \mathcal{P}_1(X_t | X_{t-1}, D_t, \sigma_{\psi_t}^2, \theta_t) \mathcal{P}_2(D_t | d_t, \phi) f(X_{t-1}, X^*). \end{aligned}$$

We expand it to all $t \in \tau_N \cup \tau_M$ (see Appendix) to have

$$f(X_1, X_2, \dots, X_{T-1}, X^*, D_2, \dots, D_{T-1}, \theta_2, \dots, \theta_{T-1}, d_2, \dots, d_{T-1}) = \mathcal{P}_0(X_1, X^* | R_1, R_T, \sigma_R^2) \prod_{t=2}^{T-1} \mathcal{P}_1(X_t | X_{t-1}, D_t, \theta_t, \sigma_{\psi_t}^2) \mathcal{P}_2(D_t | d_t, \phi). \quad (6)$$

The function in equation 6 above pertains to one single segment of the full trajectory of the fish. Therefore, with all K segments of the trajectory, the likelihood is

$$f(X_{k_1}, X_{k_2}, \dots, X_{k_{T-1}}, X_k^*, D_{k_2}, \dots, D_{k_{T-1}}, \theta_{k_2}, \dots, \theta_{k_{T-1}}, d_{k_2}, \dots, d_{k_{T-1}}) = \prod_{k=1}^K \left(\mathcal{P}_0(X_{k_1}, X_{k_T} | R_{k_1}, R_{k_T}, \sigma_R^2) \prod_{t=2}^{T-1} \mathcal{P}_1(X_{k_t} | X_{k_{t-1}}, D_{k_t}, \theta_{k_t}, \sigma_{\psi_t}^2) \mathcal{P}_2(D_{k_t} | d_{k_t}, \phi) \right)$$

where k_t denotes the t -th time step of the k -th segment of the fish trajectory, and $X_{k_1} = X_{k-1}^*$ for all $k > 1$, i.e. the fish's new starting location is its previous end location.

5 Simulation Study

We conduct a simulation study to validate the proposed imputation model. To this end, we apply the method to two selected fish with acoustic tag numbers 18453 and 18434. One fish exhibited migratory behavior, while the other fish's recorded movement was almost stationary. The timeline for each fish varies. The first fish's time period is from September 12, 2017, to September 1, 2018, while the second fish's period is from September 23, 2017, to October 10, 2017. Since no environmental covariates or population interactions are considered in this current model, and these two fish trajectories are imputed independently, the difference in timelines has no effect on our imputations. The time points are currently considered the daily locations of the fish. Specifically, the first fish was detected at time points of $t = 1, 5, 10, 12$, and by receiver numbers 45, 32, 19, 13. This indicates that the fish was detected at these four receivers over four different days within a span of twelve consecutive days, and thus, $K = 3$, $T_{k=1} = 5$, $T_{k=2} = 6$, and $T_{k=3} = 3$. Similarly, the second fish was detected at $t = 1, 7, 18$, and by receivers 44, 30, 26; $K = 2$, $T_{k=1} = 7$, and $T_{k=2} = 12$.

We demonstrate the effectiveness of the model for these different fish behaviors using parametric bootstrap sampling along with likelihood filtering to obtain the most credible estimated paths [3]. Moreover, we utilize the prior predictive simulation with relatively uninformative prior distributions for the non-stochastic parameters. While we do not restrict the prior distributions to take on any specific parameter value, we carefully select hyperparameters that meet our desired criteria. Thus, we select prior distributions for the parameters that reflect the prior knowledge and theoretical considerations regarding the described method. For α , we use $\Gamma(10, 10)$ to ensure a positive value with a mean of 1, indicating weak prior informativeness. For ϕ , a *Lognormal*(0.5, 100) is used to achieve a positive value with a wide range of variability. The γ parameter follows a $\mathcal{N}(1, 10)$ distribution, centered at 1 to have a reasonable initial value for $\sigma_{\psi_t}^2$. Lastly, σ_R^2 is modeled as *Inv - Gamma*(3, 0.00298) to achieve a variance value that ensures $3\mathbb{E}(\sigma_R) \approx r$. In other words, the variance accounts for the sparsity between receivers. The threshold parameter, β , is currently set at a fixed value of 3, because according to the fish direction's variability in equation 5 and exploratory data analysis, we believe that for a gap of length 3 or less, the fish direction is more directly predictable compared to longer gaps. In other words, a fish has more mobility in different directions for a gap of length 4 and more.

We initially focus on the first fish with relatively short time gaps. The fish's trajectory starts at $t = 1$ near receiver 45, then 3 days later, near receiver 32 and then the trajectory continues to receiver 19 in between before arriving at the last location at $t = 12$ near receiver 13.

To illustrate the algorithm, we consider the first fish for one iteration (Figure 1a). The large black points in this figure show the fish's simulated locations at the missing time points. The gray lines connecting these points illustrate the trajectory progression from receiver 45 to receiver 13. Thus, it is important to note that this line does not imply a linear path between the simulated points, but is intended to show a visual guide to understand the overall movement.

For example, by parametric bootstrap sampling along with likelihood filtering, we repeat the simulation algorithm for 5000 iterations and keep 4500 of the most probable ones (i.e. with 90% highest likelihood values). Hence, Figure 1b shows 4500 iterations for fish ID 18453. Additionally, in Figure 2, a heatmap of the same iterations is shown. This heatmap is available in Appendix C with a higher resolution.

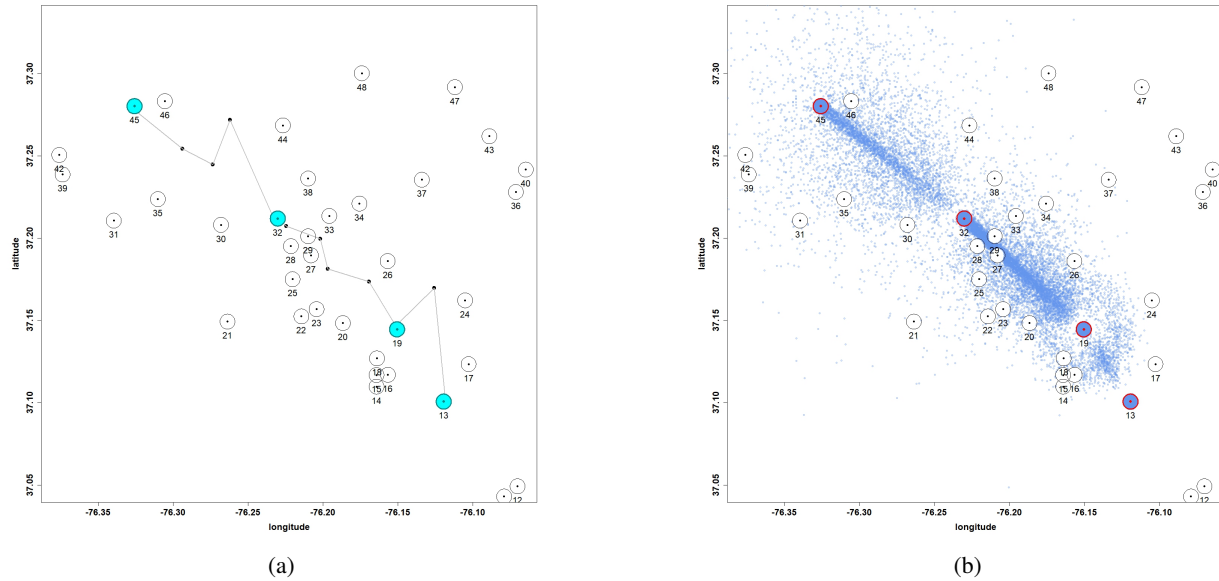


Figure 1: Comparison of one simulated trajectory (panel (a)) and 4500 simulated trajectories (panel (b)) for fish ID 18453 over 12 time steps using the proposed algorithm. The receivers that detected the fish are shown in color.



Figure 2: Heatmap corresponding to Figure 1b.

The imputation for the second fish (ID 18434) is shown in Figures 3a and 3b. Figure 3a shows the 90% most probable simulated trajectories out of 2000, while Figure 3b shows the heatmap of the same trajectories. These two figures demonstrate the reduced realism of the proposed method when larger time gaps exist. Specifically, for the 10 step gap between receivers 30 and 26, the imputed trajectories tend to follow a more linear pattern. Ecologically, cobia are known for their tendency of migratory behavior, and therefore, this simulated linearity is less realistic [2]. During longer gaps between the recorded detections, fish are expected to exhibit non-linear, multi-directional movements rather than straight paths. Hence, this example demonstrates that our current imputation method requires modification to capture the natural movement behaviors of fish over long unobserved time periods.

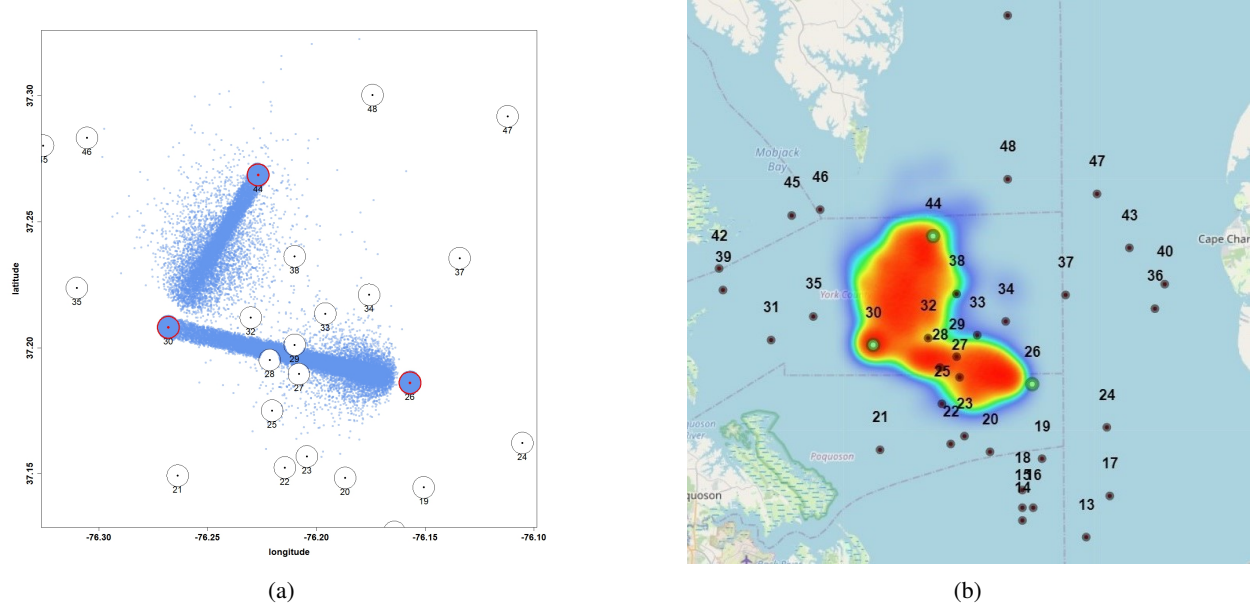


Figure 3: Simulated trajectories and heatmap. Panel (a): 4500 simulated trajectories for fish ID 18434 over 18 time steps using the proposed algorithm. Panel (b): Heatmap corresponding to panel (a).

6 Discussion

In summary, this paper focuses on the imputation of cobia movement trajectories while accounting for physical limitations due to the tracking technology (acoustic tagging), accompanied by visual validation. The challenges addressed in this paper are the structure of the data and the methods used for data collection temporally. The data are very sparse, and the actual fish location is unknown even when presence is detected. In fact, these are the complexities of tracking the fish acoustically, which lead to a lack of applicability of the common models for animal movement analysis. In our paper, we developed a new strategy to handle these challenges.

We intend to apply our algorithm to impute all fish trajectories from the full dataset ($N = 67$ fish) by [2]. The goal is to develop an inference model that also integrates relevant environmental characteristics along with the imputed data. This will improve understanding and prediction of the behavior of this fish species as well as those animals with similar movement patterns.

The hierarchically structured algorithm introduced in this paper offers a framework for independently imputing short-time gaps in the trajectory of each fish. However, the individuality of fish-specific imputations and the unavailability of the fish's actual locations do not provide the context for performing a cross-validation study.

As future work, we will extend this model by incorporating a transition probability matrix for each time step, giving us the probabilities of fish transitioning between different receivers, and therefore, the fish location predictions will allow population-level inference on which k-fold cross-validation can be employed. Additionally, we will improve the fish-specific model's applicability to more extensive time gaps by incorporating multiple layers of mixture modeling to distinguish between "lazy" and "nosy" behavior, and between resident and migratory populations.

Despite the progress in modeling techniques, several challenges remain. Data quality and quantity can be compromised by tag malfunctions or environmental interference, leading to incomplete datasets [11, 22, 1, 8]; these challenges are beyond the scope of our current work. Environmental factors such as water temperature and salinity influence fish movement and add complexity to model predictions. Furthermore, ensuring model accuracy and validation is essential to represent actual movement patterns accurately. Our inference framework (in progress) aims to incorporate these elements into the imputation method presented in this paper. We anticipate our current paper and inference framework (upon completion) to add substantial rigor to this field of research.

Acknowledgement

We gratefully acknowledge the financial support of the Virginia Sea Grant through a graduate fellowship awarded to M.A. which made this research possible. We also extend our appreciation to Dr. Daniel P. Crear (Inter-American Tropical Tuna Commission) and Dr. Kevin Weng (Virginia Institute of Marine Science) for providing the necessary resources and their guidance during this work.

References

- [1] S.J. Cooke, S.G. Hinch, M. Wikelski, R.D. Andrews, L.J. Kuchel, T.G. Wolcott, and P.J. Butler. Biotelemetry: a mechanistic approach to ecology. *Trends in Ecology & Evolution*, 19(6):334–343, 2004.
- [2] D.P. Crear, B.E. Watkins, V.S. Saba, J.E. Graves, D.R. Jensen, A.J. Hobday, and K.C. Weng. Contemporary and future distributions of cobia, *Rachycentron canadum*. *Diversity and Distributions*, 26(8):1002–1015, June 2020.
- [3] A.C. Davison and D.V. Hinkley. *Bootstrap Methods and Their Application*. Cambridge University Press, 1997.
- [4] M. Dawkins. Melded bayesian inference for stochastic theoretical models with applications in agent based modelling, 2017. Graduated with High Honours.
- [5] R.M. Dorazio and M. Price. State-space models to infer movements and behavior of fish detected in a spatial array of acoustic receivers. *Canadian Journal of Fisheries and Aquatic Sciences*, 76(4):543–550, 2019.
- [6] Mingzhu Fu, Robert S. Cantrell, Chris Cosner, and Lei Zhang. A functional response model of animal movement: Spatiotemporal behavior of animal populations. *Journal of Mathematical Biology*, 71(1):233–258, 2015.
- [7] Nancy Heckman and John Ross. Functional data analysis of animal movement trajectories. *Journal of Agricultural, Biological, and Environmental Statistics*, 22(3):377–399, 2017.
- [8] M.R. Heupel, J.M. Semmens, and A.J. Hobday. Automated acoustic tracking of aquatic animals: scales, design and deployment of listening station arrays. *Marine and Freshwater Research*, 57(1):1–13, 2006.
- [9] N.E. Humphries, N. Queiroz, J.R.M. Dyer, N.G. Pade, M.K. Musyl, and K.M. Schaefer et al. Environmental context explains lévy and brownian movement patterns of marine predators. *Nature*, 465:1066–1069, 2010.
- [10] G. Huse, J. Giske, and A.G.V. Salvanes. Modeling individual-based populations: A review and introduction. In *Handbook of Fish and Fisheries*, pages 228–248. Blackwell, Oxford, 2002.
- [11] N.E. Hussey, S.T. Kessel, K. Aarestrup, S.J. Cooke, P.D. Cowley, A.T. Fisk, R.G. Harcourt, K.N. Holland, S.J. Iverson, J.F. Kocik, et al. Aquatic animal telemetry: a panoramic window into the underwater world. *Science*, 348(6240):1255642, 2015.
- [12] D.R. Jensen and J.E. Graves. Movements, habitat utilization, and post-release survival of cobia (*rachycentron canadum*) that summer in virginia waters assessed using pop-up satellite archival tags. *Animal Biotelemetry*, 8(24), 2020.
- [13] D.I. Jonsen, R.A. Myers, and J.M. Flemming. Meta-analysis of animal movement using state-space models. *Ecology*, 84(11):3055–3063, 2003.
- [14] I.D. Jonsen, J.M. Flemming, and R.A. Myers. Robust state-space modeling of animal movement data. *Ecology*, 86(11):2874–2880, 2005.
- [15] R. Joo, S. Bertrand, J. Tam, and R. Fablet. Hidden markov models: the best models for forager movements. *PLoS One*, 8(8):e71246, Aug 23 2013.
- [16] J.R. Norris. *Markov Chains*. Cambridge University Press, 1998.
- [17] T.A. Patterson, M. Basson, M.V. Bravington, and J.S. Gunn. Classifying movement behaviour in relation to environmental conditions using hidden markov models. *Journal of Animal Ecology*, 78(6):1113–1123, 2009.
- [18] T.A. Patterson, L. Thomas, C. Wilcox, O. Ovaskainen, and J. Matthiopoulos. State-space models of individual animal movement. *Trends in Ecology & Evolution*, 23(2):87–94, 2008.
- [19] S.F. Railsback. Concepts from complex adaptive systems as a framework for individual-based modeling. *Ecological Modeling*, 139:47–62, 2001.
- [20] S.M. Ross. *Introduction to Probability Models*. Academic Press, 11th edition, 2014.
- [21] D.W. Sims, E.J. Southall, N.E. Humphries, G.C. Hays, C.J.A. Bradshaw, and J.W. Pitchford et al. Scaling laws of marine predator search behavior. *Nature*, 451:1098–1102, 2008.
- [22] E.B. Thorstad, F. Whoriskey, A.H. Rikardsen, and K. Aarestrup. Aquatic animal telemetry. *Marine Ecology Progress Series*, 482:1–3, 2013.

A Second-order Taylor Expansion for \mathbf{Z}

$$\text{For } \mathbf{Z} = \begin{bmatrix} Z^{(1)} = \cos(\theta^*) \\ Z^{(2)} = \sin(\theta^*) \end{bmatrix},$$

$$\begin{aligned} Z^{(1)} &= \cos \theta^* \\ &\approx \cos \theta - (\sin \theta)(\theta^* - \theta) - \frac{1}{2}(\cos \theta)(\theta^* - \theta)^2 \\ &\approx (\sin \theta)(\theta^* - \theta) - \cos \theta \left(1 - \frac{(\theta^* - \theta)^2}{2} \right) \\ \mathbb{E}(Z^{(1)}) &\approx \cos \theta \left(1 - \frac{\sigma_\psi^2}{2} \right) \\ \text{Var}(Z^{(1)}) &\approx (\sin \theta)^2 \sigma_\psi^2 + \frac{1}{2}(\cos \theta)^2 \sigma_\psi^4 \end{aligned}$$

and

$$\begin{aligned} Z^{(2)} &= \sin \theta^* \\ &\approx \sin \theta + (\cos \theta)(\theta^* - \theta) - \frac{1}{2}(\sin \theta)(\theta^* - \theta)^2 \\ &\approx \cos \theta(\theta^* - \theta) - (\sin \theta) \left(1 - \frac{(\theta^* - \theta)^2}{2} \right) \\ \mathbb{E}(Z^{(2)}) &\approx (\sin \theta) \left(1 - \frac{\sigma_\psi^2}{2} \right) \\ \text{Var}(Z^{(2)}) &\approx (\cos \theta)^2 \sigma_\psi^2 + \frac{1}{2}(\sin \theta)^2 \sigma_\psi^4 \end{aligned}$$

and by letting $C = \cos(\theta)$ and $S = \sin(\theta)$, we have

$$\begin{aligned} \text{Cov}(Z^{(1)}, Z^{(2)}) &\approx -SC\sigma_\psi^2 + \frac{1}{2}SC\sigma_\psi^4 \\ \begin{bmatrix} Z^{(1)} \\ Z^{(2)} \end{bmatrix} &\overset{\text{approx}}{\sim} \mathbf{N}_2 \left(\begin{bmatrix} \cos(\theta) - \frac{1}{2}\cos(\theta)\sigma_\psi^2 \\ \sin(\theta) - \frac{1}{2}\sin(\theta)\sigma_\psi^2 \end{bmatrix}, \sigma_\psi^2 \begin{bmatrix} S^2 + \frac{1}{2}C^2\sigma_\psi^2 & -SC + \frac{1}{2}SC\sigma_\psi^2 \\ -SC + \frac{1}{2}SC\sigma_\psi^2 & C^2 + \frac{1}{2}S^2\sigma_\psi^2 \end{bmatrix} \right). \end{aligned}$$

B Joint Distribution of Stochastic Terms for $\mathbf{T}=4$

Assume the trajectory lacks observations at time steps $t = 2, 3$. Thus, $X_4 = X^*$, and

$$\begin{aligned} &\mathcal{P}[X_1, X_2, X_3, X_4, \theta_2, \theta_3, D_2, D_3, d_2, d_3] \\ &= \mathcal{P}[X_3 | X_1, X_2, X_4, \theta_2, \theta_3, D_2, D_3, d_2, d_3] \times \\ &\quad \mathcal{P}[D_3 | X_1, X_2, X_4, \theta_2, \theta_3, D_2, d_2, d_3] \times \\ &\quad \mathcal{P}[d_3, \theta_3 | X_1, X_2, X_4, \theta_2, D_2, d_2] \times \\ &\quad \mathcal{P}[X_2 | X_1, X_4, \theta_2, D_2, d_2] \times \\ &\quad \mathcal{P}[D_2 | X_1, X_4, \theta_2, d_2] \times \\ &\quad \mathcal{P}[d_2, \theta_2 | X_1, X_4] \times \\ &\quad \mathcal{P}[X_1] \mathcal{P}[X_4] \\ &= \mathcal{P}[X_3 | X_2, D_3, \theta_3] \mathcal{P}[D_3 | d_3] \times \\ &\quad \mathcal{P}[X_2 | X_1, D_2, \theta_2] \mathcal{P}[D_2 | d_2] \times \\ &\quad \mathcal{P}[X_1] \mathcal{P}[X_4] \end{aligned}$$

Note that $\mathcal{P}[d_3, \theta_3 | X_1, X_2, X_4, \theta_2, D_2, d_2] = \mathcal{P}[d_3, \theta_3 | X_2, X_4]$ drops out of the likelihood due to non-stochasticity. The same applies to $\mathcal{P}[d_2, \theta_2 | X_1, X_4]$.

C High resolution heat map

Download Figure 2 in high resolution HTML format at <https://go.wm.edu/4YYgLP>.